

## Dynamic process of angular distortion between aluminum and titanium alloys with TIG welding

WANG Rui(王蕊), LIANG Zhen-xin(梁振新), ZHANG Jian-xun(张建勋)

State Key Laboratory for Mechanical Behavior of Materials, School of Materials Science and Engineering,  
Xi'an Jiaotong University, Xi'an 710049, China

Received 24 April 2007; accepted 6 July 2007

**Abstract:** The dynamic process of welding angular distortion in the overlaying welding of 5A12 aluminum alloy and BT20 titanium alloy was investigated. Information of dynamic distortion was got via self-made welding dynamic measuring system. Research results show that the characteristics of dynamic distortions at various positions of the plate edge parallel to the weld of 5A12 and BT20 alloy are different. Comparison between 5A12 and BT20 alloy shows that transverse shrinkage and downward longitudinal bending are main factors influencing the dynamic angular distortion processes of 5A12 and BT20 alloy under welding heat input of 0.32 kJ/mm. The angular distortion of 5A12 alloy is completely inverted with welding heat input increasing to 0.4 kJ/mm, and the position of weld center and buckling distortion become the primary factors.

**Key words:** dynamic distortion; 5A12 aluminum alloy; BT20 titanium alloy; critical state

### 1 Introduction

Welding distortion is one of the most important problems in welding fabrication. In principle, there are four fundamental types of distortion, namely the longitudinal shrinkage, the transverse shrinkage and the angular distortions in two directions, and various forms of distortions are produced as their combination[1–2]. The distortions of welded structures lead typically to uncertainty in design and manufacture and to high rectification costs. These drawbacks are especially evident in thin plates[3–5]. For a given material, the magnitude of distortion depends primarily on the specific thermal energy input of the welding progress. In Refs.[6–7], the authors put forward a simplified finite element simulation method of out-of-plane distortion. The “mismatched thermal strain”(MTS) and “thermal contraction strain”(TCS) were used to calculate the longitudinal and transverse deformations. The heat input rate, weld penetration and fusion zone shape are the main factors for longitudinal contraction deformation and angular distortion, respectively. It is concluded that the peak temperature at a given transverse location is the

primary driver for the distortion process. In order to predict the initial shape more accurately, gravity and support conditions should be considered.

It is well known that titanium and aluminum alloys are used extensively due to their attractive combination of high specific strength and excellent corrosion resistance. So behaviors of welding on titanium and aluminum alloys attract considerably interest in the world[8–14]. Most research results are dedicated to the theoretical formula and computing model, and discuss the effects of welding parameters and material properties on welding residual stresses and distortions[15–18].

In this work, a new measuring approach is adopted to obtain information of dynamic angular distortions and welding temperature accurately. The characteristics of dynamic angular distortions and thermal cycle at different welding positions of aluminum and titanium alloys are studied. The research results can provide some references for predicting and controlling welding distortion.

### 2 Experimental

The overlaying welding tests were carried out by

using TIG welding to study dynamic process of 5A12 aluminum alloy and BT20 titanium alloy. The chemical compositions of two alloys are listed in Table 1.

The specimens were positioned on the clamping system, constraining a well-defined region (Fig.1). The dynamic temperature and distortion were determined by self-made real time welding dynamic measuring system, as investigated in a previous work[19]. The processing conditions were as follows: the size of the plate 200 mm × 160 mm × 2.5 mm, welding current 60 A, and voltage 11 V. The welding speed was varied from 12.5 cm/min to 10 cm/min. The schematic illustration of test is shown in Fig.2. Four displacement sensors locate at pre-defined positions (including position 1, position 2, position 3, and position 4, which are arranged at the plate edge parallel to the weld) of the plate bottom, 20 mm away from the front edge of plate, and 30, 100, 140 and 190 mm away from welding start edge. Temperature measurement was conducted at position 5, which is 5 mm away from weld.

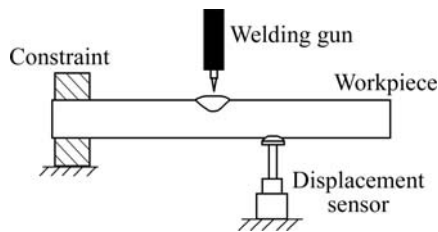


Fig.1 Schematic diagram of experimental system

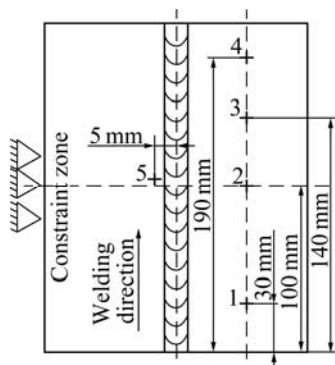


Fig.2 Experiment layout

The temperature-dependent material properties of two alloys are presented in Fig.3. The temperature-dependent material properties play decisive role on transient temperature, stress and distortion during

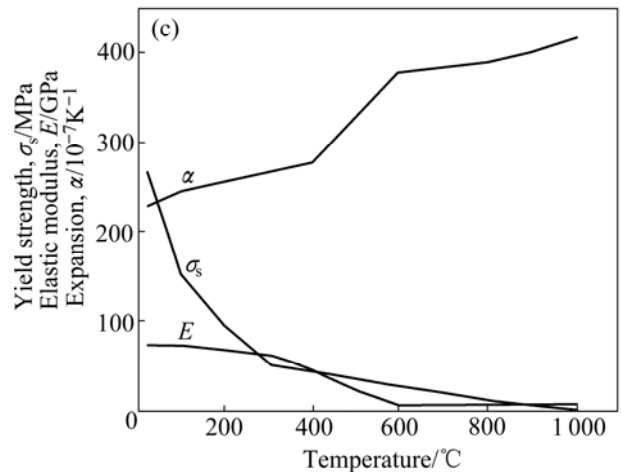
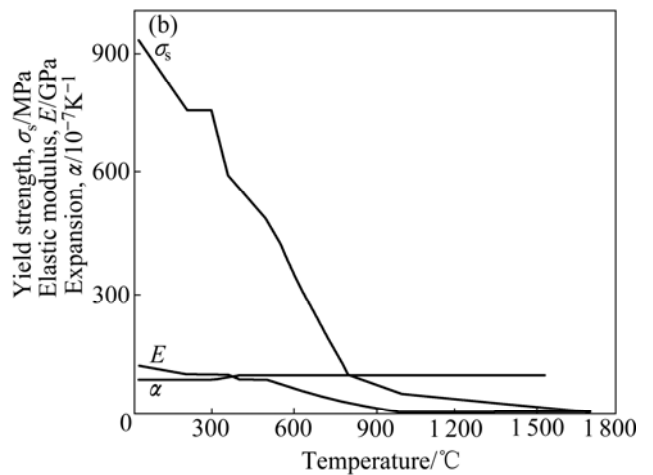
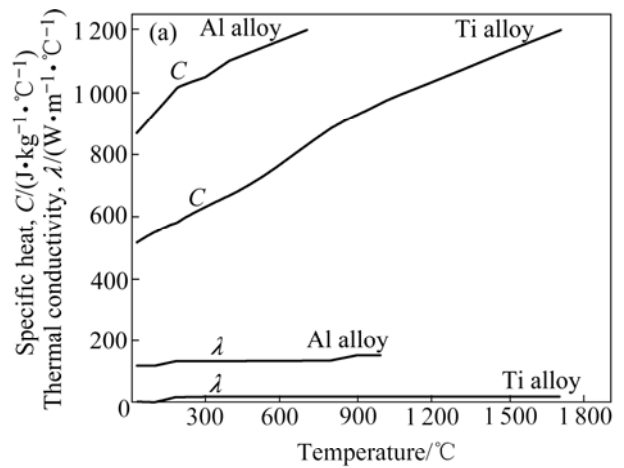


Fig.3 Variation of material properties with temperature of two alloys: (a) Thermal properties of Ti and Al alloy; (b) Mechanical properties of Ti alloy; (c) Mechanical properties of Al alloy

Table 1 Main compositions of two alloys (mass fraction, %)

Sample	Ti	Al	Mo	V	Fe	Si	Zr	C	N	H	O
BT20	Bal.	5.5-7.0	0.5-2.0	0.8-2.5	0.3	0.15	1.5-2.5	0.1	0.05	0.015	0.15
Sample	Al	Mg	Cu	Ni	Fe	Si	Mn	Ti	Zn	Zr	Cr
5A12	Bal.	8.3-9.6	0.05	0.10	0.05	0.3	0.4-0.8	0.05-0.15	0.20	-	-

welding process[20–21]. The thermal conductivity has influence on distribution of transient temperature field, and the yielding stress has significant influence on the residual stress and distortion.

### 3 Results and discussion

The dynamic distortion characteristics of two alloys are shown in Fig.4. Curves 1–4 show the displacements at positions 1–4, respectively. As shown in Fig.4(a), the dynamic distortion tendencies of BT20 at different positions are similar. After welding starts, the temperature of weld metal is elevated, causing expansion of volume, but this behavior is hindered by the base metal. So the transverse shrinkage distortion is generated, and the displacements slowly increase. With the moving of welding torch, the metal after welding starts to cool, which cause transverse and longitudinal shrinkage of weld metal, and the increase of displacements. The maximum distortions maintain until room temperature. This indicates that the transverse shrinkage and downward longitudinal bending are the main factors inducing dynamic angular distortion in welding process. For Curve 1 and Curve 4, the maximum distortion is achieved at 400 s. For Curve 2 and Curve 3, the time is 600 s.

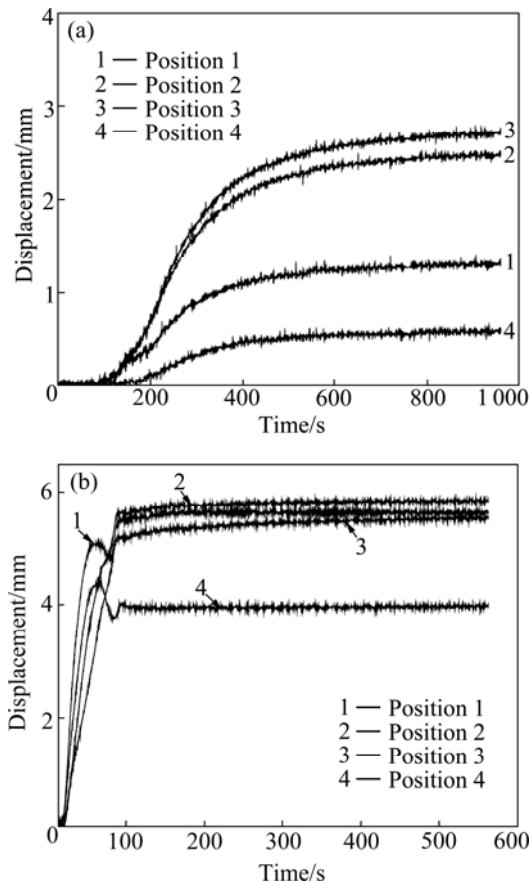


**Fig.4** Dynamic distortion results of two alloys: (a) Titanium alloy BT20; (b) Aluminum alloy 5A12

Distortion characteristics of aluminum alloy are shown in Fig.4(b). It needs 50 s to achieve the first peak value for curve 1 and curve 4. With welding time increasing, upward longitudinal bending is obviously strengthened, the angular distortion is counterbalanced, and the displacements are reduced. The displacements slightly increase again after 30 s, but the displacements are smaller than the initial maximum value. For Curve 2 and Curve 3, the upward longitudinal bending is not obvious. The transverse shrinkage and downward longitudinal bending are the main factors inducing dynamic angular distortion.

The characteristics of distortions at different positions are complex. The dynamic distortion progresses of two alloys are shown in Fig.5. It can be observed from Fig.5(a) that the distortion of BT20 alloy at the initial stage is bowling. With time increasing to 100 s, the displacements of initial region (position 1, position 2) are higher than those of ending region (position 3, position 4), and the distortion becomes buckling. This stage is the critical state of distortion. At the last stage, the distortion tendency is completely reversed. It changes to arch shape and the displacements at the middle (position 2 and position 3) of the plate are

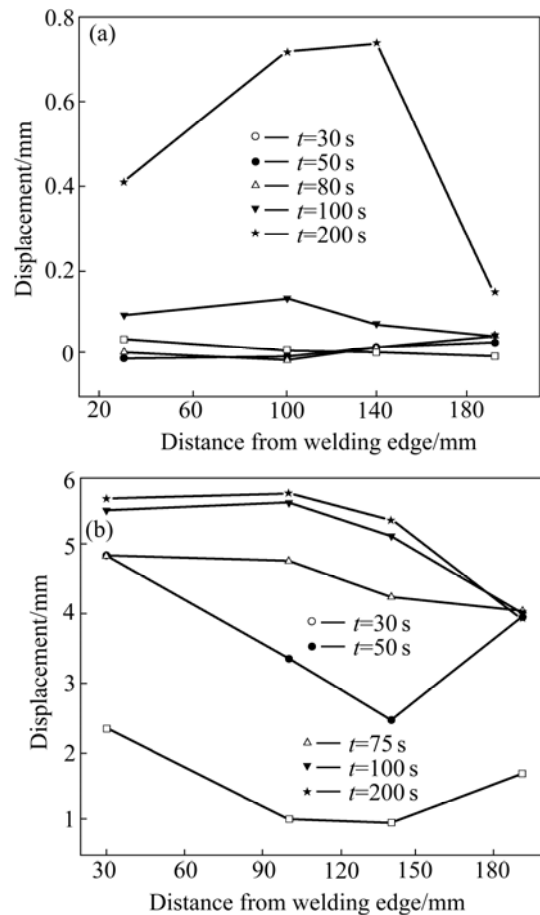


**Fig.5** Displacements of measured points along edge parallel to weld line at different time: (a) Titanium alloy BT20; (b) Aluminum alloy 5A12

larger than those of the edges (position 1, position 4).

The dynamic distortion progresses of 5A12 alloy are shown in Fig.5(b). At the initial stage, the distortion is bowling. The displacements at the edges of the plate are higher than those of the middle. With time increasing to 75 s, the displacements of initial region are higher than those of ending region, and the distortion is buckling. This stage is the critical state for 5A12 alloy. At the last stage, the distortion tendency is reversed. It changes to arch shape.

The dynamic distortion results of two alloys show that the critical state of distortion for BT20 and 5A12 alloy occurs at 100 s and 75 s, respectively. Compared with titanium alloy, the steady state of aluminum alloy pre-occurs.

The temperature distribution and dynamic distortions of two alloys at different positions are shown in Fig.6. It can be seen from Fig.6(a) that the change tendencies of thermal cycle curves of two alloys are different. The temperature of 5A12 alloy increases after welding, but it keeps stable for BT20 alloy. The temperature of 5A12 alloy increases slowly compared with BT20 alloy, due to the fact that the high thermal conductivity results in the function of pre-heating of far-plane to the researched-plane. The temperature gradient of BT20 alloy is greater than that of 5A12 alloy and the equilibrium temperature of 5A12 alloy is higher than that of BT20 alloy. So the larger distortion can be produced under the condition of high equilibrium temperature[22].

The displacements of the position 1 are shown in Fig.6(b). The expansion coefficient of aluminum alloy is higher than that of titanium alloy (Fig.3). The displacement of 5A12 alloy rapidly increases until 50 s, then decreases. But the distortion tendency keeps in short duration and then rapidly rises again until reaching the maximum value. For BT20 alloy, there is not distortion until 50 s. And the distortion slowly increases until reaching the maximum value after 400 s. Because the physical properties of two alloys are different, the thermal expansion coefficient of aluminum alloy is high, and the yield stress is small, the displacement of 5A12 alloy is higher than that of BT20 alloy.

The displacements of position 2 are shown in Fig.6(c). The distortion tendencies of two alloys are similar. But the change speed of 5A12 alloy is extremely quick because of the high thermal expansion coefficient. The dynamic displacements are still mainly influenced by the transverse shrinkage.

The dynamic distortion processes of BT20 and 5A12 alloys with heat input increasing from 0.32 kJ/mm to 0.4 kJ/mm are shown in Fig.7. As shown in Fig.7(a), the transverse shrinkage of BT20 alloy causes the displacement rapidly to increase, whereas upward longi-

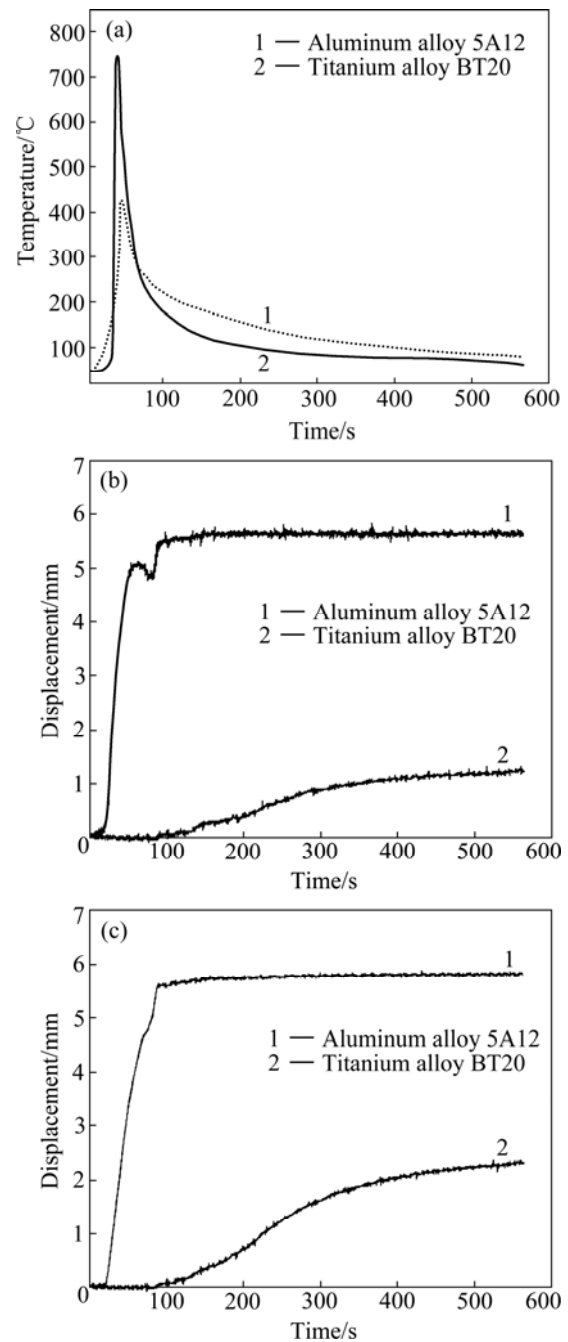


**Fig.6** Curves of dynamic distortion of two alloys: (a) Thermal cycle at 5 mm away from weld; (b) Distortion at position 1; (c) Distortion at position 2

tudinal bending increases greater with the welding heat input increasing, and the displacement decreases. But this tendency keeps for about 50 s and the displacement continually increases. Under the combined effect of transverse shrinkage and longitudinal shrinkage, the maximum value of displacement is achieved. The displacement at position 1 is the smallest, and the displacement sequentially decreases along welding direction. This distortion tendency is similar with that of 5A12 alloy, as shown in Fig.4(b).

As shown in Fig.7(b), the displacements of the

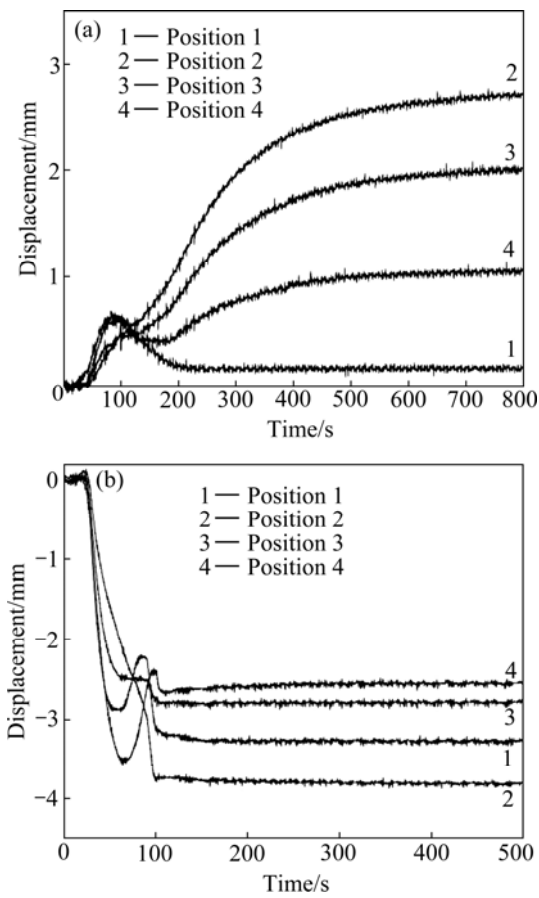


**Fig.7** Dynamic distortion with heat input increasing: (a) Titanium alloy BT20; (b) Aluminum alloy 5A12

5A12 alloy rapidly decrease after welding. The downward angular distortion is formed. While the metal of weld completely melts, excess penetration bead is formed. The center of weld moves down. Although the partial dropping tendency is counterbalanced by upward angular distortion, the position of weld center is the primary factor affecting the dynamic angular distortion.

The dynamic distortion progresses of two alloys under welding heat input of 0.4 kJ/mm are shown in Fig.8. At the initial stage, the distortion of BT20 alloy behaves as buckling. The displacements of ending region (position 3, position 4) are higher than those of initial region (position 1, position 2). The distortion changes from buckling to bowling at 80 s. The critical state for BT20 alloy is 150 s. The displacements are the same to the initial stage that the displacements of ending region are a little higher than those of initial region. At the last stage, the distortion distribution is completely reversed to arch shape so that the displacements of the middle of the plate (position 2 and position 3) are higher than those of the edges (position 1 and position 4).

For 5A12 alloy, the total tendency of distortion is downward angular distortion. As welding starts, the distortion is in arch shape, and the displacements of

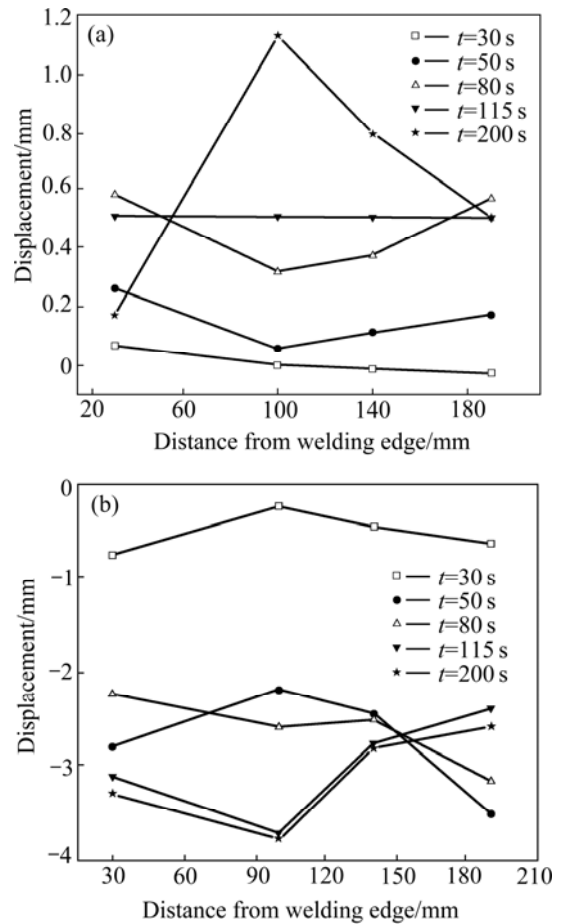


**Fig.8** Displacements of measured points along edge parallel to weld line at different time: (a) Titanium alloy BT20; (b) Aluminum alloy 5A12

middle of the plate are higher than those of the edges. When time increases to 80 s, the distortion changes from arch to buckling.

The dynamic distortion results of two alloys show that the critical states of distortion for titanium alloy and aluminum alloy occur at 115 s and 80 s, respectively. The steady state of aluminum alloy pre-occurs. With welding heat input increasing, the time of two alloys reaching steady state also increases.

With the heat input increasing to 0.4 kJ/mm, thermal cycle curves and dynamic distortions of two alloys are shown in Fig.9. It can be seen from Fig.9(a) that with the heat input increasing, the peak temperature and temperature gradient of two alloys increase.

The displacements at position 1 are shown in Fig.9(b). The displacement of titanium alloy rapidly changes in 100 s. After 100 s, the displacement starts to drop. The displacement no longer changes after 200 s. Finally, small residual distortion is formed. The displacement of aluminum alloy is reversed under welding heat input of 0.4 kJ/mm. The distortion changes to downward angular distortion. The displacement increases in 80 s, then the thermal expansion is hindered

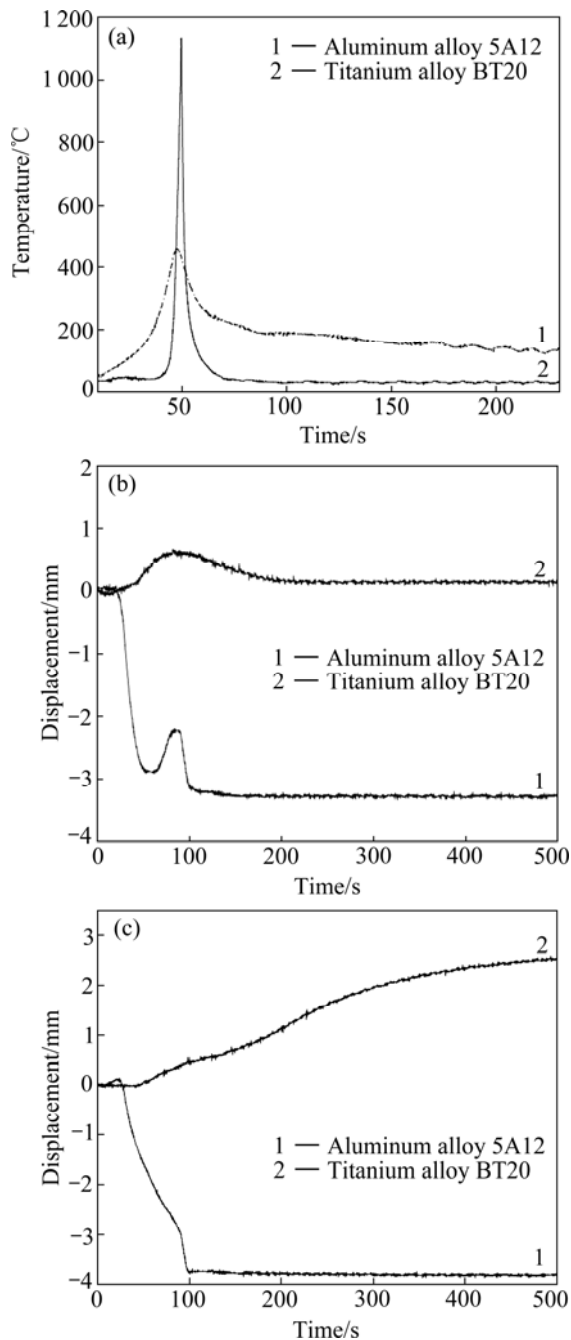


**Fig.9** Dynamic distortion and thermal cycle of two alloys with increasing heat input: (a) Thermal cycles at 5 mm away from weld center; (b) Position 1; (c) Position 2

and a compressive thermal stress can be induced. The change of the displacement between 80 s and 100 s is mutually counterbalanced, which no longer changes after 100 s. The final displacement is far smaller than the initial displacement.

The displacements at the position 2 are shown in Fig.9(c). With the heat input increasing to 0.4 kJ/mm, the displacement of titanium alloy increases because of transverse shrinkage. The displacement change tendency for aluminum alloy is completely opposite to titanium alloy. The displacement drops until achieving the

maximum displacement at 100 s.

## 4 Conclusions

1) The equilibrium temperature of aluminum alloy 5A12 is higher than that of titanium alloy BT20. Temperature gradient of titanium alloy BT20 increases with the increase of welding heat input.

2) The characteristics of dynamic distortions of two alloys are different. When the welding heat input is equal to 0.32 kJ/mm, the dynamic distortion process of titanium alloy BT20 includes three stages: bowling, buckling, and arch. The tendency is the same as aluminum alloy 5A12. When welding heat input is equal to 0.4 kJ/mm, the change tendency of titanium alloy BT20 is buckling, bowling and arch, whereas only two tendencies, such as arch and buckling, occur for aluminum alloy 5A12. The time of steady state for two alloys increases with welding heat input increasing.

3) With heat input increasing to 0.4 kJ/mm, main factors influencing the dynamic angular distortion change from transverse shrinkage and downward longitudinal bending to position of weld for aluminum alloy 5A12. The dynamic distortion tendency of titanium alloy BT20 is similar to aluminum alloy 5A12 under welding heat input of 0.32 kJ/mm.

4) The distortion of aluminum alloy is higher than that of titanium alloy. The peak value of welding distortion of aluminum alloy appears early.

## References

- [1] RADAJ D. Heat effects of welding; temperature field, residual stress, distortion [M]. New York: Springer-Verlag Berlin Heidelberg, 1992.
- [2] MURAKAWA H, LIANG Wei, DENG De-an, KOUTAROU I. Prediction of welding distortion of large scale structure using inherent deformation [C]// Proceedings of Welding Science and Engineering, Xi'an: 2005: 1-11.
- [3] MICHALERIS P, DEBICCARI A. Prediction of welding distortion [J]. Welding Journal, 1997, 76: 172-181.
- [4] ASLE ZAEEM M, NAMI M R, KADUVAR M H. Prediction of welding buckling distortion in a thin wall aluminum T joint [J]. Computational Materials Science, 2007, 38: 588-594.
- [5] DHINGRA A K, MURPHY C L. Numerical simulation of welding-induced distortion in thin-walled structures [J]. Science and Technology of Welding and Joining, 2005, 10(5): 528-536.
- [6] CAMILLERI D, COMLEKCI T, GRAY T G F. Computational prediction of out-of-plane welding distortion and experimental investigation [J]. Journal of Strain Analysis, 2005, 40(2): 161-176.
- [7] MOLLICONE P, CAMILLERI D, GRAY T G F, COMLEKCI T. Simple thermo-elastic-plastic models for welding distortion simulation [J]. Journal of Materials Processing Technology, 2006, 176: 77-86.
- [8] PAPAZOGLU V J, MASUBCHI K. Analysis and control of distortion in welded aluminum structures [J]. Welding Journal, 1978, 57(9): 251-262.
- [9] LI Zhang, GOBBI L, NORRIS I, ZOLOTOSKY S, RICHTER K H. Laser welding technique for titanium alloy sheet [J]. Journal of

- Materials Processing Technology, 1997, 65(1/3): 203–208.
- [10] HE Xiao-dong, ZHANG Jian-xun, GONG Shui-li, LI J H. Residual stress measurements with the hole-drilling technique in the joints by the laser and TIG welding for a thin plate of titanium alloy [J]. Material Science, 2003(12): 7–10. (in Chinese)
- [11] MASUBUCHI K. Prediction and control of residual stresses and distortion in welded structures [J]. Trans JWRI, 1996, 25(2): 53–67.
- [12] HE Xiao-dong, ZHANG Jian-xun, PEI Yi, GONG Shui-li. Test of residual stress in laser beam welding and TIG welding joints of aeronautical titanium alloy plate [J]. Welding & Joining, 2003(10): 26–29. (in Chinese)
- [13] MARYA M, EDWARDS G R. A study on the laser forming of near-alpha and metastable beta titanium alloy sheets [J]. Journal of Materials Processing Technology, 2001, 108: 376–383.
- [14] TERASAKI T, YAMAKAWA D. Study of welding deformation and welding residual stress generated in pure titanium joints [J]. Welding International, 2003, 17(11): 864–869.
- [15] MICHALERIS P, SUN X. Finite element analysis of thermal tensioning techniques mitigating weld buckling distortion [J]. Welding Journal, 1997, 76(11): 451–457.
- [16] PARK J U, LEE H W, BANG H S. effect of mechanical constraints on angular distortion of welding joints [J]. Science and Technology of Welding and Joining, 2002, 7(4): 232–239.
- [17] MIYASAKA F, YAMANE Y, OHJI T. Development of circumferential TIG welding process model: A simulation model for welding of pipe and plate [J]. Science and Technology of Welding and Joining, 2005, 10(5): 521–527.
- [18] GERY D, LONG H, MAROPOULOS P. Effects of welding speed, energy input and heat source distribution on temperature variations in butt joint welding [J]. Journal of Materials Processing Technology, 2005, 167: 393–401.
- [19] WANG Rui, ZHANG Jian-xun, LIANG Zhen-xin. Development of a measurement system for dynamic welding distortion and temperature cycle [J]. Welding and Joining, 2006(1): 27–31.
- [20] ZHU X K, CHAO Y J. Effects of temperature-dependent material properties on welding simulation [J]. Computers and Structures, 2002, 80: 967–976.
- [21] CANAS J, PICON R, PARIS F, BLAZQUEZ A, MARIN J C. A simplified numerical analysis of residual stresses in aluminum welded plates [J]. Computers and Structures, 1996, 58(1): 59–69.
- [22] LIN Y C, CHOU C P. Residual stress due to parallel heat welding in small specimens of type 304 stainless steel [J]. Materials Science and Technology, 1992, 8(9): 837–840.

(Edited by YANG Bing)